First demonstration of the FLASH effect with ultrahigh dose-rate high energy X-rays

Feng Gao[1,+], Yiwei Yang[2,+], Hongyu Zhu[3,+], JianXin Wang[4], Dexin Xiao[4], Zheng Zhou[4], Tangzhi Dai[1], Yu Zhang[1], Gang Feng[1], Jie Li[1], Binwei Lin[1], Gang Xie[5], Qi Ke[5], Kui Zhou[4], Peng Li[4], Xuming Sheng[4], Hanbin Wang[4], Longgang Yan[4], Chenglong Lao[4], Ming Li[4], Yanhua Lu[4], Menxue Chen[4], Jianheng Zhao[4], Song Feng[6], Xiaobo Du[1,*], and Dai Wu[4,*]

[1]Oncology Department of Mianyang Central Hospital, Mianyang, 621000, China
[2]Institute of Nuclear Physics and Chemistry, China Academy of Engineering Physics, Mianyang, 621900, China
[3]Department of Radiation Oncology, Sun Yat-sen University Cancer Center, State Key Laboratory of Oncology in South China, Collaborative Innovation Center for Cancer Medicine, Guangzhou 510060, China
[4]Institute of Applied Electronics, China Academy of Engineering Physics, Mianyang, 621900, China
[5]Pathology Department of Mianyang Central Hospital, Mianyang, 621000, China
[6]School of Nuclear Science and Technology, University of South China, Hengyang, 421001, China
[*]corresponding authors: duxiaobo2005@126.com, wudai04@gmail.com
[+]these authors contributed equally to this work

ABSTRACT

The ultrahigh dose-rate (FLASH) radiotherapy , which is efficient in tumor control while sparing healthy tissue, has attracted intensive attention due to its revolutionary application prospect. This so-called FLASH effect has been reported in preclinical experiments with electrons, kilo-voltage X-rays, and protons, thus making FLASH a promising revolutionary radiotherapy modality. High energy X-ray (HEX) should be the ideal radiation type for clinical applications of FLASH due to its advantages in deep penetration, small divergence, and cost-friendly. In this work, we report the first implementation of HEXs with ultrahigh dose-rate (HEX-FLASH) and corresponding application of *in vivo* study of the FLASH effect produced by a high-current (10 mA), high-energy (6-8 MeV) superconducting linac. Joint measurements using radiochromic film, scintillator and Fast Current Transformer device validated that a maximum dose rate of over 1000 Gy/s was achieved in the mice and the mean value within several square centimeters keeps higher than 50 Gy/s within a depth of over 15 cm. The performance of the present HEX can satisfy the requirement of the FLASH study on animals. Breast cancer (EMT6) inoculated into BAL b/c mice was found efficiently controlled by HEX-FLASH. The radio-protective effect of normal tissue was observed on the C57BL/6 mice after thorax/abdomen irradiation by HEX-FLASH. Theoretical analyses of cellular response following HEX-FLASH irradiation based on the radiolytic oxygen depletion hypothesis were performed to interpret experimental results and future experiment design. This work provided the first demonstration of the FLASH effect triggered by HEX, which paved the way for future preclinical research and clinical application of HEX-FLASH.

Introduction

Cancer is the first or second leading cause of death of human beings before age 70 in 91 of 172 countries, while ranks third or fourth in an additional 22 countries[1]. Radiotherapy is one of the most widely used and effective anti-tumor therapy methods[2], and 60-70% of cancer patients need radiotherapy during the whole treatment process[3].

In the history of radiotherapy for more than 70 years[4], the whole world has been trying to find an ideal radiotherapy method, which needs to be effective, safe, and affordable. From 2-dimensional radiotherapy to intensity-modulated radiotherapy, the volume of tumor target could be more accurately limited, thus reducing the radiated dose to adjacent organs.Because of the development from intensity-modulated radiation therapy (IMRT) to intensity-modulated arc therapy (IMAT)[5,6], radiotherapy's time cost was further shortened. With the improvement of image-guided technology in radiotherapy, radiologists can deliver a more massive single dose to the tumor to achieve a better tumor control rate. In addition, benefiting from the "Bragg peak" of proton and heavy-ion in the organism[7–9], radiologists can deliver larger doses to tumors while reducing the radiation dose to surrounding normal tissues. However, so far, radiologists have not been able to develop superior radiotherapy technology. The conventional dose rate radiotherapy (CONV 0.07–0.1 Gy/s)[10]is a double-edged sword. CONV radiotherapy can shrink the tumor but, at the same time, lead to radiation-induced toxicities to normal tissue. Normal tissue complications limit the dose delivered to the tumor, which means that a tumor cannot always be killed completely, thus decreasing radiotherapy's efficacy.

Therefore, killing the tumor while protecting normal tissues has always been the main challenge of radiotherapy.

More than five decades ago, some protective effects of the normal tissue by ultrahigh dose rate were found and discussed[11], but the same protective effect on isolated HeLa cells[12] limited the clinical imagination of this phenomenon. The re-recognition of this effect is the discovery that tumor cells in living mice can be suppressed by ultrahigh dose rate radiation[13] in 2014. Since then, this new ultrahigh dose-rate (FLASH, $\geq$40 Gy/s) modality showed a remarkable healthy-tissue-sparing effect in many preclinical studies without impacting the overall treatment efficacy (called FLASH effect) compared with conventional dose-rate (CONV, $\leq$0.03 Gy/s) radiotherapy[14]. The total course of treatment of FLASH radiotherapy can be implemented within several milliseconds, being time and tumor control efficient while protecting the normal tissue. Therefore, FLASH will point to the revolutionary way for the ideal radiotherapy. Although the mechanism is still unclear and some negative results have been reported[15], several FLASH-RT studies on animals showed an obvious FLASH effect[13,14,16–22], and the first patient treatment in Switzerland also got a satisfactory result[23]. Based on the aforementioned studies, the U.S. Food and Drug Administration (FDA) approved the research device exemption for the first FLASH-RT clinical trial[24].

Electrons[10,13,15,19–21,25–28], kilo-voltage (keV) X-rays[18,29] and proton[30–32] have been utilized in FLASH preclinical research; however, those modalities are not ideal in clinical application. Electrons and keV X-rays are usually used to treat superficial tumor sites, but not suitable for tumors in the deep body, such as lung cancer, breast cancer, colorectal cancer, prostate cancer, due to their limited penetration powers. FLASH proton can be used to treat the deep tumor, but the high cost of treatment determines only a few patients can afford it. What about the most widely used rays –High energy X-ray (HEX)? HEX has the obvious advantage of deep penetration, small divergence, and good cost-effectiveness, which is the most suitable ray for clinical FLASH radiotherapy. Unfortunately, because of the vast difficulty to establish HEX of high dose-rate (HEX-FLASH), it has not yet been available in FLASH research either *in vitro* or *in vivo*.

This work reports the first demonstration of FLASH effect triggered by HEX on platform called PARTER (Platform for Advanced RadioThErapy Research). In PARTER, high energy, high average current electron beam (6 - 8 MeV, > 5 mA) was produced by the GaAs photocathode and superconducting linac. The highest instantaneous dose-rates in the mice was up to 4 MGy/s, corresponding to a mean dose rate of over 1000 Gy/s. EMT6 tumor homografts on BALb/c mice were irradiated by HEX in FLASH and CONV to examine the tumor control efficiency of these two modalities. The thorax and abdomen of healthy C57BL/6 mice were irradiated to evaluate the FLASH effect in the normal tissue brought by HEX. Furthermore, we have performed the first theoretical analysis of the FLASH effect of HEX based on the radiolytic oxygen depletion (ROD), which is a leading explanation to interpret the FLASH effect.

Results

HEX-FLASH was implemented using the superconducting linac

High energy electron beam produced by the superconducting linac on CTFEL was guided to bombard rotating tungsten target on PARTER and converted to bremsstrahlung X-rays for FLASH irradiation(Fig. 1a, 1b, 1c). This procedure was essentially the same as that in the CONV radiotherapy machine, thus the energy spectra of the HEX on PARTER is similar with that on CONV radiotherapy machine, which had been checked by Monte Carlo computing (MCC)[33].

As a critical parameter, the dose rate has been measured carefully to verify the implementation of FLASH . The absolute dose measured by medical radiochromic films (EBT3) showed good agreement (discrepancy<4%) with MCC results based on the electron number given by Fast Current Transformer (FCT) devices, and the time structure measured by FCT and $CeBr_3$ scintillator (Fig. 1d, 1e)agreed with the linac character. The time history of the dose rate given by the scintillator monitor and FCT showed good agreement(<1%), while around 5% discrepancy appeared after $\sim$1ms when the beam power was higher than 40 kW (Fig. 1f). It was probably induced by the beam energy attenuation and should be corrected in the total dose. Both measurements and MCC results showed that in an irradiation field of 6 cm in diameter, the dose rate produced by the HEX on PARTER was higher than 50 Gy/s at a depth of up to over 15 centimeters in water(Fig. 1g). The percentage depth dose (PDD) in the sample was adjustable by changing the beam current (1-10 mA) and energy (6-8 MV) of the superconducting linac. In our experiments, the maximum dose rate in mice was up to over 1000 Gy/s. As the depth increases, dose rates dropped rapidly, although the dose uniformity in the irradiation field was improved. When both the collimator window and the target area were set as 2 cm $\times$ 2 cm, the dose uniformity ratio (DUR) was 1.43 and 1.25 at the depth of 4 mm and 6 mm, respectively. (Fig. 1h, 1i). MCC showed that $\sim$ 9% of the dose deposited at the surface layer (0-2 cm) was produced by leaked high-energy electrons when beam energy was set to 8 MeV, and it was less than 1% if the depth was over 2 cm or the energy was 6 MeV. Dose calibration was carried out before every biological experiment to verify the status of PARTER and reconfirm the correlation coefficients between dose rate, beam current and scintillator current.

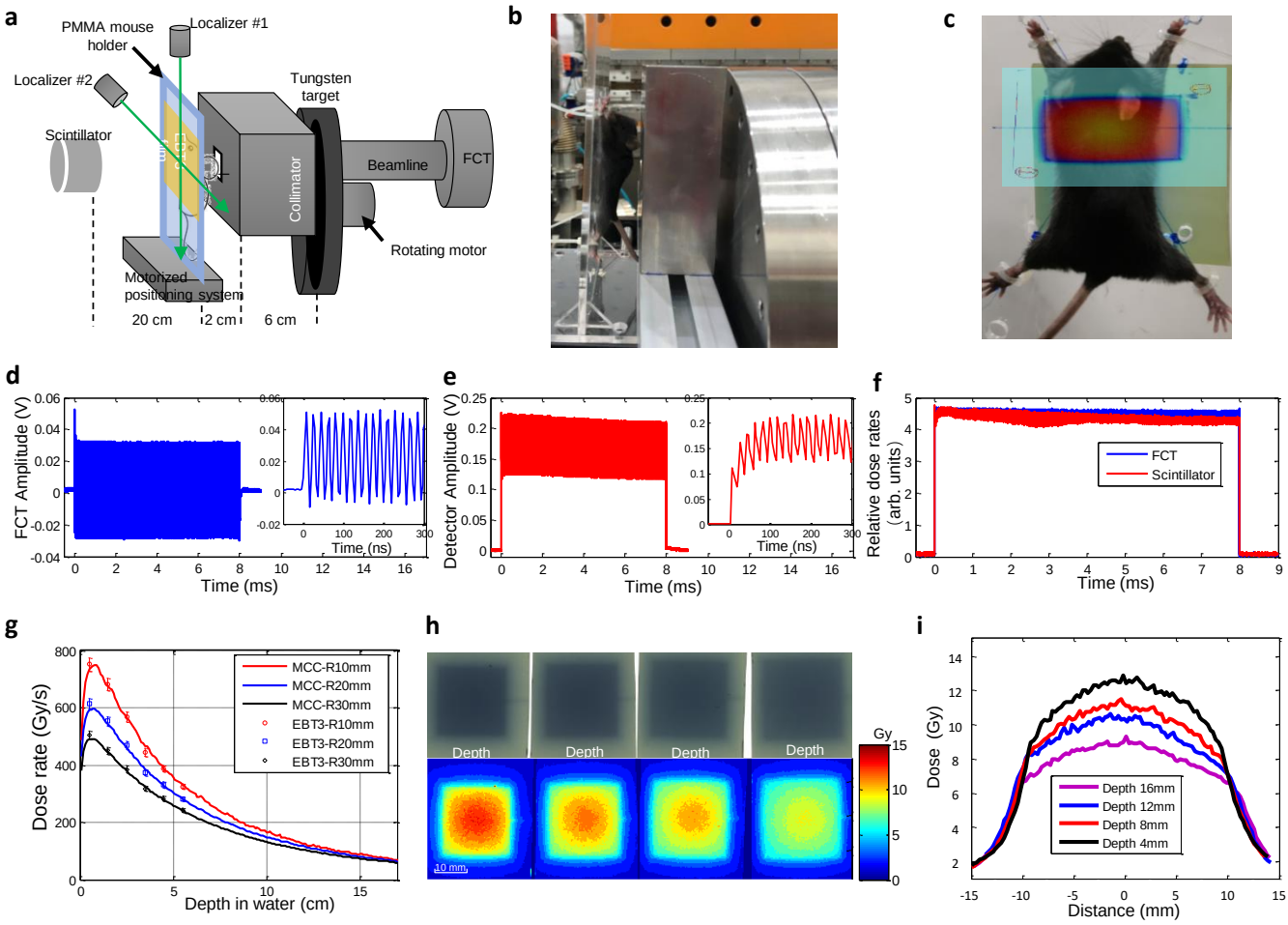

Figure 1. Parameter and result of the basic HEX-FLASH experiment on PARTER. a The schematic diagram of the HEX FLASH study on PARTER. **b** A mouse was fixed on the PMMA holder when exposed to FLASH irradiation, and EBT3 film was stuck on the backside of the holder **c** to verify the location of the irradiation field on the mouse and assist with dose measurement. **d** The current and pulse width of the linac was measured by FCTs installed on the beamline with a time resolution of nanoseconds, and **e, f** the time history was compared with that given by the scintillator. For measurement of dose rate and distribution, six EBT3 films were mounted at various depths down to 45 mm in the solid water phantom located at the sample position, 7 cm behind the rear surface of target chamber, and irradiation by HEX corresponding to a beam of 7 MeV/3.8 mA.**g** The mean dose rates within three different radii (R10 mm, R20 mm and R30 mm) in these EBT3 films agree with MCC results based on the beam current given by FCT in 1% at most of the points but larger discrepancy (∼3%) appears near the surface. Smaller radius shows higher mean dose rates because of the center-edge dose attenuation and the maximum mean dose rate within R10 mm, achieved at 0.5 cm depth, was ∼750 Gy/s. The dose distribution in the phantom was measured before every biological experiment.**h** Four EBT3 films were mounted in 4-16 mm depth of a PMMA phantom behind a collimator window (2 cm × 2 cm) and were irradiated for 15 ms by HEX corresponding to 6 MeV / 5.35 mA beam. **i** 2D dose distribution and profile on x-direction in each film

HEX-FLASH radiotherapy is as efficient as CONV radiotherapy in controlling subcutaneous homografts tumor in mice

A dose of 18 Gy was delivered to subcutaneous homografts tumor in a single fraction by HEX-FLASH (900 Gy/s $\times$ 20ms) with linac presetting to 8 MV/4.4 mA. CONV irradiation (0.1 Gy/s) was performed in the same faction with the total dose 15 Gy to the other 15 tumor-bearing mice.

According to the observation during 63 days post-irradiation (pi), the growth rates of tumors irradiated by FLASH or CONV were slower compared with control group. The slowest growth rate of tumor volume was achieved by FLASH radiotherapy, and the difference of tumor volume between the three groups became bigger as time went by. The tumor volume in control group exceeded 40000 mm^3 after 40 days pi, whereas the maximum of volume in CONV and FLASH groups was $\sim$ 30000 mm^3 and $\sim$ 15000 mm^3 during our whole observation(Fig. 2b). The difference between CONV and FLASH group was statistically significant (p=0.0002 in one-way ANOVA). A significant difference in volume between the three groups was also proved by one-way ANOVA analysis in which F = 25.14, P <0.0001.

Significantly different (p <0.005) was also observed between the survival curves of the three groups of mice(Fig. 2c), in which similar median survival time appeared in FLASH group (55 days) and CONV group (59.5 days) while control group got only 35.5 days.

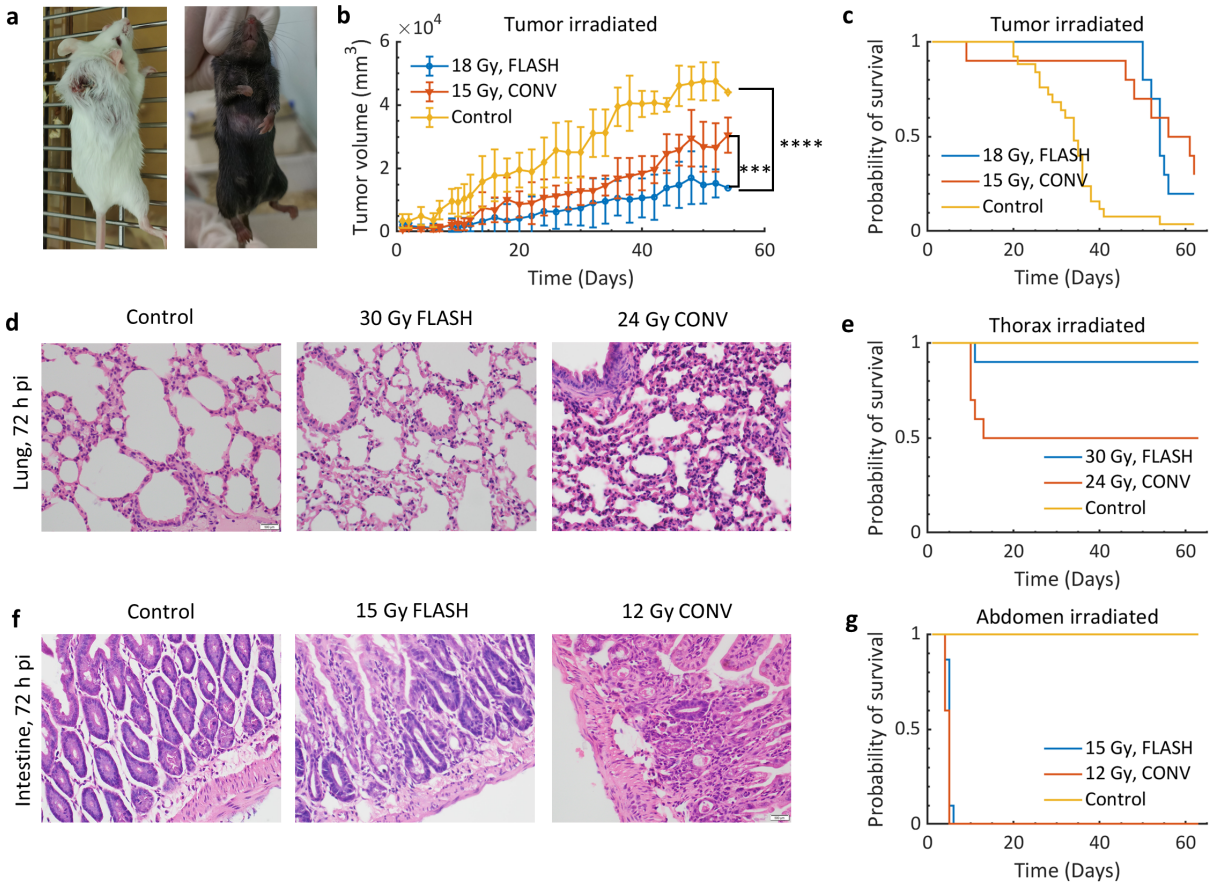

Figure 2. **a** The tumor-bearing BAL b/c mice (left) and healthy C57BL/6 mouse (right) used in this study. **b** Evolution of EMT6 tumor homografts in BAL b/c mice. **c** Survival curves of tumor-bearing BAL b/c mice of the control group, after 18 Gy FLASH and 15 Gy CONV irradiation. **d** Hematoxylin-eosin-saffron (HES) of the lung tissue of healthy C57BL/6 mice under microscope. **e** Survival curves of healthy C57BL/6 mice of the control group, after 30 Gy FLASH and 24 Gy CONV irradiation. **f** HES of the small intestine tissue of healthy C57BL/6 mice under microscope. **g** Survival curves of healthy C57BL/6 mice of the control group, after 15 Gy FLASH and 12 Gy CONV irradiation.P values were derived from one-way repeated ANOVA: *P < 0.05, **P < 0.01, ***P < 0.001, ****P < 0.0001.

HEX-FLASH radiotherapy leads to less radiation-induced damage than CONV radiotherapy in lungs and intestines

In lung research, fifty-eight C57BL/6 mice were divided into three groups, control group, thorax group irradiated by 30-Gy FLASH (1200 Gy/s× 25 ms) or 24-Gy CONV group (0.1 Gy/s) in a single fraction. Here the dose of the CONV group was preset to 20% lower than the FLASH group to ensure the actual dose received by the FLASH group was not less than the CONV group even if the superconducting accelerator appeared any power fluctuation during FLASH irradiation, which was proved negligible by the actual measurement. Five mice were sampled in each group at 72h pi for pathological examination while the rest were fed for survival observation. Hematoxylin-eosin-saffron (HES) staining of lung sections showed that alveolar structures in the FLASH group were similar to the control group, whereas obviously more alveolar structures broke and inflammatory cells infiltrated appeared in the lung sections of the CONV group (Fig. 2d).

Similarly, in intestine research, C57BL/6 mice were divided into two groups for irradiation. Control group was the same mice mentioned above. FLASH group and CONV group received dose of 15 Gy (937 Gy/s×16 ms) and 12 Gy (0.1 Gy/s) in a single fraction radiation to abdomen, where the dose of the CONV group was also preset to 20% lower than the FLASH group although the superconducting accelerator turned out to be stable enough.The three images show that the small intestine's basic structure still existsHowever, the inflammatory response was more severe in the pictures of the intestine section from the CONV group and the FLASH group than that in the control group, especially in the CONV group. More glandular dysplasia in the Flash group than the CONV group and neutrophil infiltration could be seen in the CONV group. (Fig. 2f)

Mice were fed for more than two months in order to get the survival data. For the thorax irradiated mice(Fig. 2e), the survival rate was 100% in the control group, 90% in the FLASH group and 50% in the CONV group at the end of the observation. The median survival time was not reached in the FLASH group and 38 days in the CONV group. There was a statistically significant difference (P=0.038) in survival among the three groups. The Hard Ratio (HR) was 0.19, 95% CI [0.035 – 1.010], p = 0.0486 for the FLASH group and CONV group, which means the risk of death decreased by 81% in the FLASH group compared with CONV group. For the abdomen irradiated mice(Fig. 2g), the survival rate was also 100% in control group at 63 days pi but all the mice in the FLASH group and CONV group died at 4-5 days pi with no statistically significant difference.

Theoretic cellular response analysis of the FLASH effect based on the ROD hypothesis

The amount of oxygen depleted in cells (pO_2=7.5 mmHg before irradiation) due to the HEX-FLASH irradiation was simulated to be L_{ROD} =0.196 mmHg/Gy, reduced oxygen tension in cells leads to fewer DNA damages and higher cell survival fractions (SFs). Fig. 3a presents the oxygen enhancement ratio (OER), which is defined as the ratio of the dose in anoxia to the dose in air required to achieve a given biological endpoint (e.g., a defined cell SF), as a function of oxygen tension (Scattered data points were extracted from previous experiments[34–38] as references). Higher OER values at lower oxygen tensions mean cells are more radioresistant. When a dose of 10, 20, or 30 Gy was delivered to cells with an initial pO_2=7.5 mmHg, intracellular oxygen tension decreased, and the OER value increased from 1.41 to 1.52, 1.69, and 2.06, respectively. Fig. 3b presents the Chinese hamster ovary (CHO) cell SF curve under the FLASH irradiation and the CONV irradiation; an enlarged difference of SFs between FLASH and CONV irradiation can be observed with the increase of dose. Though we considered a different cell line in the theoretic analysis, it shows a consistent radioprotective effect of normal cells trend under the FLASH irradiation.

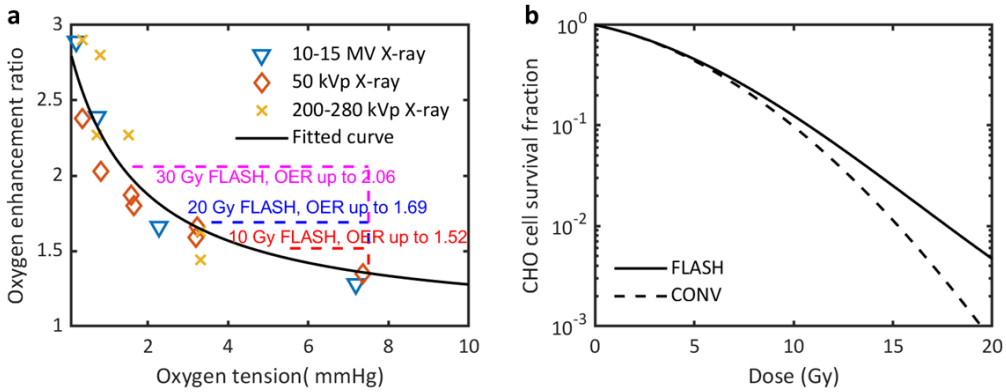

Figure 3. **a** The oxygen enhancement ratio (OER) as a function of oxygen tension (Data were extracted from references[34–38]). FLASH irradiation can lead to a rapid oxygen depletion in cells, resulting in an increment of OER values (increase of radioresistant). **b** Chinese hamster ovary (CHO) cell survival curves under the FLASH and CONV irradiation.

Discussion

HEX-FLASH was unarguably implemented on PARTER owing to the high current beam provided by the advanced superconducting linac at CTFEL, although the performance of the prototype is still some distance from clinical application. As two critical parameters of HEX-FLASH, energy and dose rate has been verified by repeated measurements and careful MCC. Base on the HEX-FLASH, several preliminary but critical investigations of physiological responses *in vivo* were performed to verify whether the HEX can trigger remarkable FLASH effect in mice. Our results demonstrated that, compared with CONV, HEX-FLASH protected lungs and intestines from radiation-induced damage while keeping an equal efficiency in tumor control. This work is a huge milestone in the history of FLASH and even radiotherapy because this revolutionary modality was implemented and proven effective via a clinically applicable approach.

To ensure high enough dose rate, the source-surface distance (SSD) on present PARTER platform is ∼6-20 cm, much closer than that on CONV radiotherapy machine(∼1.2 m), which means a higher divergence of the X-rays and more secondary electrons will arrive at the surface of the sample. Moreover, high-strength magnets for removing leaked electrons was off-line on PARTER in the FLASH experiment to protect the mice from magnetic damage considering the small SSD. These aforementioned factors jointly caused the peak of the PDD curve of our HEX-FLASH (0.7-1 cm) slightly deviated from that in CONV (∼1.5 cm) of same beam energy. In present HEX-FLASH irradiation with the beam energy of the linac setting to 8 MV, ∼ 10% of the dose delivered to mice came from leaked electrons while it was negligible (<1%) in 6-MV irradiation. The magnets will be optional in future FLASH experiments, although leaked electrons would not affect the result in the preclinical HEX-FLASH study. Therefore, the recommended beam energy in the HEX-FLASH study on present PARTER is 6 MV corresponding to a maximum dose rate of ∼800 Gy/s in mice.

A fundamental problem faced by the present PARTER prototype is, due to the missing of flattening filter, dose uniformity which can be improved only by increasing the SSD now. In the preclinical experiment, the SSD was set to 6-20 cm owe to the small field size for mice/cell irradiation and, according to MCC, the longest SSD on the prototype is 60 cm, beyond which the dose rates will be lower than the 50 Gy/s then fall out of the FLASH range. The effective SSD will further decrease to around 40 cm when a filter is added to uniform the dose distribution to clinical requirement but reduce dose rate by tens of percent. Fortunately, all the performance of PARTER prototype can satisfy the needs of present HEX-FLASH study on animals, and the superconducting linac at CTFEL will upgrade to phase II with power up to over 100 kW then provide beam with current over three times as much as it is now, by then the effective SSD for FLASH will be up to 100 cm thus very close to the clinical level.

Another critically important problem is precise dosimetric system that presently consist of EBT3 film, FCT beam monitor and scintillator dosimeter. This system can jointly determined the dose in ±5%, higher than that in CONV (generally ±2%) but acceptable for a prototype.The real-time dose rate in sample during irradiation computed according to the beam current given by FCT showed some discrepancy with that given by the scintillator, especially early in the macro-pulse with high beam current. It is not yet clear whether the discrepancy is due to energy attenuation of the linac or efficiency change of the scintillator, so we can only avoid it by using a relatively low beam current. Different kinds of dosimeters will be used in our following work to help finding the reason and improve the dose precision. In addition, new EBT-XD film will be put into use to extend its dose range to over 40 Gy.Compared with CONV radiotherapy, the ultra-short irradiation time is a significant advantage of FLASH but also a big challenge for real-time adjustment of linac characters. In present HEX-FLASH study, the energy/current of the linac and width of the macro-pulse are preset according to calibration and computing, but the inevitable power fluctuation of the linac during real irradiation leads the actual dose to deviate from design (usually ±5%). Although we had considered this fluctuation in dose design and large sample number can also counteract some of the effect in animal experiments, the interaction between dosimetric system and linac must be put on our agendas for more precise experiment and future clinical application.

In the following anti-tumor effect experiment, we observed a significant difference in the volume of tumors in three groups, essentially consistent with the results reported by Vincent Favaudon[13]. HEX-FLASH radiotherapy showed a surprisingly excellent effect in tumor controlling, although the subcutaneous tumor volume was a little bit oversize when irradiated due to a long waiting time for the setting up of PARTER. However, this apparently better effect in controlling tumors by HEX-FLASH radiotherapy probably comes from its 20% higher dose than the CONV radiotherapy. So our conclusion is the effect of HEX-FLASH radiotherapy and CONV radiotherapu turn out to be similar in controlling tumor, and more rigorous comparison experiments will be carried out soon to confirm it further. Besides, the tumor-bearing mice should be killed when the tumor volume exceeded 3, 000 mm^3 but, considering it a rare work , we continued the feeding for more data on survival. By the way, we collected the data on tumor volume. The curve of tumor volume stopped at 54 days pi because the data after that will be statistically insignificant due to many mice died on that day, while the survival curve is not impacted. We have observed an exact protective effect of lung tissue in the FLASH group even the total dose was 25% higher than the CONV group. The result is a powerful evidence that HEX-FLASH radiotherapy has protective effect to the normal tissue. However, in the intestine radiotherapy experiment, when the total dose of the FLASH group was still 25% higher than the CONV group, the protective effect of HEX-FLASH radiotherapy disappeared. The explanation for this result might be following:firstly, the tolerance dose of different tissues to radiation is different, such as the median lethal dose (LD50) of the small intestine is significantly

lower than lung's in CONV radiotherapy[39–41]. Due to the poor radio-tolerance of the small intestine, the dose delivered to the abdomen in the CONV group was its lethal dose. Moreover, when 25% higher dose was delivered to the FLASH group, the mice died sharply thus the protective effect of FLASH was masked over. To eliminate the interference brought by lethal dose and inconsistency of total dose in FLASH radiotherapy and CONV radiotherapy, BAL b/c mice with better radio-tolerance[41] were used in the additional experiments, in which the total doses were strictly controlled and verified.

Equal dose (30 Gy) was delivered to the mice' bilateral thorax in a single fraction by FLASH (700 Gy/s) and CONV (0.1 Gy/s) irradiation, and the same procedure was performed on mice' whole abdomen irradiation except the total dose was set to 12 Gy. The result showed that the survival time of mice irradiated by bilateral thorax and whole abdomen was both prolonged, probably due to the better radio-tolerance of mice. The median survival time of the thorax-irradiated mice in FLASH group (120 days) and CONV group (86 days) (Fig.S2a) were statistically different (HR 0.187; 95%CI, 0.044 –0.803, P<0.0001). For the abdomen irradiation, FLASH group won an obviously better survival curve than the CONV group in which all mice lived less than 10 days pi. (Fig.S2b). 62.5% of the mice in the FLASH group were still alive when we stopped observation, thus the median survival time of the FLASH group could not be achieved. Although it was undoubtedly that survival time of mice in the FLASH group was much higher than that in the CONV group (7 days), the difference in survival between the two groups was not statistically significant(HR 0.369;95% CI, 0.113—1.202; P =0.0735). Even so,the trend toward survival benefit brought by FLASH radiotherapy forcefully proved the FLASH effect of HEX.

In this study, a theoretic analysis of cellular response following HEX-FLASH irradiation was performed based on the OFH hypothesis, which is the leading candidate to explain the FLASH effect. The L_{ROD} =0.196 mmHg/Gy was determined for HEX-FLASH, this allowed us to determine cellular pO_2 post irradiation, and evaluate the change of oxygen-dependent radiosensitivity based on the general relationship between OER and oxygen tension (see Fig. 3a). Besides, current calculation results were obtained with single pulse fractionation, which was the dose delivery regimen adopted in experiments of this study and most of the previous publications[10,14]. However, the FLASH effect triggered by different pulse fractionation regimens is of research interest[42]. The calculation method adopted in this work was also applied to analyze cellular responses under different fractionations, this serves as a reference for future experiment design (please see the supplementary material).

In summary, three part of works were conducted in this study. Firstly, the PARTER system produced the first FLASH-HEX and its physical properties were confirmed. Moreover, positive FLASH effect triggered by HEX was observed in this study. Besides, theoretic analyses were provided for the interpretation of experimental results and future experiment design. The current study provided the basis for future scientific researches and clinical applications of HEX in FLASH radiotherapy.

Methods

Irradiation Devices

The FLASH irradiation of high energy X-ray was carried out on the PARTER platform at CTFEL facility, Chengdu, China, of which the superconducting linac can produce 6-8 MeV electrons with adjustable mean current up to 10 mA while keeping the energy spread less than 0.2% (RMS, measured when beam energy was 8.2 MeV). Continuous electron micro-pulses with FWHM of $\sim$5 ps, during which the instantaneous current is around 20A, are produced by the linac with a period of 18.5 ns then guided to bombard tungsten (3 mm in thickness) to generate HEX via bremsstrahlung. Users can freely adjust the start and end time of these continuous micro-pulses by controlling the cathode driving laser to construct a macro-pulse which is generally tens or hundreds of milliseconds

The HEX, after collimated by purpose-built lead collimators, horizontally irradiated the particular parts of the mice vertically fixed on the multi-hole PMMA plate. The SSD was adjustable from 6 cm to over 1 m but the recommended range is 6-20 cm for FLASH study. The parameters of the linac in each irradiation was preset according to the dose computing and calibration before mice irradiation. For comparison, irradiation of CONV dose-rates were carried out using clinical 6 MV linac ELEKTA Precise(Elekta AB, Stockholm, Sweden) in the Mianyang Central Hospital after FLASH irradiation.

Dosimetry

Gafchromic^{TM} EBT3 radiochromic film (Ashland Inc., Covington, Kentucky, USA) was used for absolute dose measurement. Before FLASH experiment, EBT3 film was calibrated using a clinical 6MeV linac ELEKTA Precise(Elekta AB, Stockholm, Sweden) and a farmer ionization chamber FC-65G (IBA Dosimetry GmbH, No.1463) associated with a IBA DOSE1 electrometer. The chamber was verified by China National Institute of Measurement and Testing Technology so traceable to international standards. The EBT3 film and ionization chamber were put at the same position in a solid water phantom and irradiated by the ELEKTA Precise. The RGB value of the EBT3 film was scanned using Epson Expression 10000XL (Seiko Epson Corporation, Japan) 24 hours after irradiation and corresponded to the dose value given by DOSE1.

A $CeBr_3$ scintillator detector was used as a relative dosimetry system because $CeBr_3$ is not a organic material and meanwhile scintillator dosemetry is still a new technology for medical use. This scintillator has high X-ray detection efficiency, short raise ($\sim$ 1 ns) and decay ($\sim$ 20 ns) time, which make it be a good approach to see very detailed time structure of the radiation

pulse. A phototube was installed behind the scintillator to convert its optical signal into electrical one which was recorded by a Tektronix MSO44 high-speed oscilloscope (Tektronix, USA) at around 1 GHz sampling frequency.

Two Fast Current Transformer (FCT) devices, named FCT1 and FCT2, were installed on the accelerator for nondestructive measurement of pulsed beam current. As a general device of the accelerator, FCT1 has been calibrated in terms of electron beam current by the CTFEL team. A Tektronix DPO4104B high-speed oscilloscope (Tektronix, USA) was used to acquire and recorded the FCT1 signals at around 1 GHz sampling frequency. FCT2 was a dedicated device of PARTER installed at the downstream of the beamline, less than one meter from the target, to monitor the beam current on the tungsten target. The same Tektronix MSO44 oscilloscope used for $CeBr_3$ scintillator shared a channel to record the FCT2 signal which was used for relative electron current monitoring only because it has not calibrated yet.All recorded signals were off-line processed by Matlab^R 2009 program (MathWorks, USA) and over 99% agreement between FCT1 and FCT2 was achieved.

As a general procedure, MCC was carried out using GEANT4[43] platform to compute the dose distribution in consideration of the clear enough structure of our PARTER platform, mainly consisting of the bremsstrahlung target, collimator and sample. As an important input of the Monte Carlo code, the accurate parameters of the electron beam were given by the advanced superconducting linac and FCT devices. These accurate structure and parameters can ensure the exactness and reliability of the MCC, which has been verified by several calibration experiments using EBT3 film for comparing.

Theoretic cellular response analysis of after HEX-FLASH irradiation

Theoretic analyses of the FLASH effect were performed with Monte Carlo (MC) simulation and previously developed radiobiological models to interpret experimental results. Theoretic analyses were based on the radiolytic oxygen depletion (ROD) hypothesis[10,44,45], a leading hypothesis for the radioprotective effect on normal tissue exposed to FLASH irradiation. The ROD hypothesis considers that the oxygen molecules were rapidly depleted during the FLASH irradiation and created a local radiobiological hypoxic environment, thus making cells less radiosensitive. Pratx and Kapp proposed that the hypoxic stem cells may be related to the radioprotection from ROD associated with the FLASH effect[45,46], therefore, hypoxic cells (with an oxygen tension pO_2 = 7.5 mmHg) were considered for cellular responses analyses in this work.

NASIC (Nanodosimetry Monte Carlo Simulation Code) was adopted for simulations of cellular responses after CTFEL HEX-FLASH irradiation. NASIC is a Monte Carlo track structure (MCTS) tool that supports simulations of physical and chemical reactions induced by ionization irradiations and analyses of subsequent radiobiological responses, including DNA damage and cell SFs under CONV-RT[47–50] and FLASH-RT[51]. The detailed description of MC simulation method and analysis model for different biological endpoints can be found in references[51,52].

DNA double-strand breaks (DSBs) induced by ionization radiation were assumed as the initial and most lethal lesions in the cell nucleus and positively related to cell death after irradiation. In the NASIC MC simulation, it was assumed that direct DNA damages were induced by physical reactions between incident particles and the DNA structure, and indirect DNA damages resulted from reactions between molecular oxygen (O_2) and DNA-derived radicals, which were produced by reactions between DNA structures and hydroxyl radicals (·OH). DNA DSB yield changes with the oxygen tension (pO_2) of cells and results in different cell SFs.

In this work, the initial DNA damage information and amount of oxygen depleted (L_{ROD}) under different fractionation schemes were simulated with NASIC, the dynamic evolution of pO_2 in cells and changes of final DNA damage yield as well as cell SFs were calculated following the method described in the reference[51,52] and the cell line used in analyses was Chinese hamster ovary (CHO) cell.

Animal experiment and ethics statement

We inoculated EMT6 mouse breast cancer cells into six-week-old BAL b/c female mice. We subcutaneously inoculated cancer cells into the back skin of mice. We did experiment on tumor-bearing mice when the inoculated tumor diameter was about 12 $\sim$ 15 mm, The tumor-bearing mice was divided into three groups, control group , irradiated by FLASH (1000 Gy/s) with 18 Gy/1F group, and irradiated by CONV (0.1 Gy/s) with 15 Gy/1F group. The radiation field was a square with a side length of 1.5 cm. After the mice were irradiated, we observed the mice every day and recorded the long and short diameters of tumor every other day. We observed the tumor-bearing mice for 63 days. The volume was calculated by the formula V = 0.52 $\times$ long diameter $\times$ short diameter^2. After calculating the volume of each mouse we averaged tumor volume and drew a line chart. We recorded the number of mice and whether they survived every day, and finally drew the survival curve of tumor-bearing mice.

Six-week-old C57BL/6 female mice were chosen for our normal tissue radiation experiments. The C57BL/6 female mice were divided into three groups: control group, FLASH group and CONV group. We irradiated the bilateral thorax of mice in FLASH group and CONV group, meanwhile confirmed the upper limit of thorax to be auricle's lower edge in natural condition, the lower limit was 2 centimeters downward upper limit. 20 mice in each group were exposed in either FLASH radiotherapy or CONV radiotherapy. In FLASH group, mice were irradiated by X-ray with the dose rate 1200Gy/s, and the total dose was 30 Gy. For CONV group mice were irradiated by X-ray with the dose rate 0.1 Gy/s, and the total dose was 24 Gy. For the intestine research,the C57BL/6 female mice were divided into three groups: control group (the same group mentioned above), FLASH

group and CONV group. The irradiation filed was a 2×4 cm^2 square. The upper edge is defined as the lower part of the thorax (2 cm below the lower edge of auricle) and the lower edge is 4 cm downward the bottom of thorax. 20 mice in each group were exposed in either FLASH radiotherapy or CONV radiotherapy. In FLASH group, mice were irradiated by X-ray with the dose rate 937Gy/s with the total dose was 15 Gy. In CONV group, mice were irradiated by X-ray with the dose rate 0.1 Gy/s with the total dose was 12 Gy.

After the mice were irradiated, we observed the survival of mice for 63 days.Lung tissues and small intestine tissues were obtained for pathological examination 72 hours pi respectively. We use a microscope to observe the lung tissue section with HES magnified by 200 or 400 times. At the end of observation we got the survival data for survival curve.

Statistics

In our research, We calculated the average tumor volume of tumor-bearing mice and overall survival (OS) of mice irradiated in different dose rate. Statistical analysis was performed using GraphPad Prism v.8.4.0 (GraphPad, La Jolla, CA). The balance between the FLASH-RT and CONV-RT groups was examined using the chi-square test or independent-sample t-test. Single factor analysis of variance (ANOVA) was used to analyze the changes of mean volume of tumor-bearing mice in the three groups. Survival curves were compared using the Kaplan-Meier method with a log-rank test. All statistical tests were conducted at 5% level of significance, and 95% confidence intervals (CIs) were calculated. A two-tailed P-value <0.05 indicated a statistically significant difference.

In our research, we selected C57BL/6 mice as healthy mice. The tumor-bearing mice were selected from 6-week-old BALb/c female mice. Before the experiment was carried out, animal ethics was approved by the Animal Ethics Committee of Mianyang Central Hospital. The ethics number is P2020032

Data availability

The authors declare that the data supporting the findings of this study are available within the paper and its Supplementary Information files. All other data are available from the authors upon reasonable request.

References

1. Bray, F. *et al.* Global cancer statistics 2018: Globocan estimates of incidence and mortality worldwide for 36 cancers in 185 countries. *CA: a cancer journal for clinicians* **68**, 394–424, DOI: https://doi.org/10.3322/caac.214922 (2018).
2. Steel Gordon, G. *Basic clinical radiobiology* (Edward Arnold Publication, London, 1993).
3. Baumann, M. *et al.* Radiation oncology in the era of precision medicine. *Nat. Rev. Cancer* **16**, 234, DOI: https://doi.org/10.1038/nrc.2016.18 (2016).
4. Whittum, D. H. Microwave electron linacs for oncology. *Rev. Accel. Sci. Technol.* **02**, 63–92, DOI: https://doi.org/10.1142/S1793626809000260 (2009).
5. Marta, G. N., Silva, V., Carvalho, H. D. A., Arruda, F. F. D. & Riera, R. Intensity-modulated radiation therapy for head and neck cancer: Systematic review and meta-analysis. *Radiother. Oncol. J. Eur. Soc. for Ther. Radiol. Oncol.* **110**, 9–15, DOI: https://doi.org/10.1016/j.radonc.2013.11.010 (2014).
6. Lancellotta, V., Chierchini, S., Perrucci, E., Saldi, S. & Aristei, C. Skin toxicity after chest wall/breast plus level III-IV lymph nodes treatment with helical tomotherapy. *Cancer Investig.* **36**, 1–8, DOI: https://doi.org/10.1080/07357907.2018.1545854 (2018).
7. Newhauser, W. D. & Zhang, R. The physics of proton therapy. *Phys. Medicine Biol.* **60**, R155, DOI: https://doi.org/10.1088/0031-9155/60/8/r155 (2015).
8. Colaco, R. J. *et al.* Rectal toxicity after proton therapy for prostate cancer: An analysis of outcomes of prospective studies conducted at the university of florida proton therapy institute. *Int J Radiat Oncol Biol Phys* **91**, 172–181, DOI: https://doi.org/10.1016/j.ijrobp.2014.08.353 (2015).
9. Rackwitz, T. & Debus, J. Clinical applications of proton and carbon ion therapy. *Semin. Oncol.* **46**, DOI: https://doi.org/10.1053/j.seminoncol.2019.07.005 (2019).
10. Montay-Gruel, P. *et al.* Long-term neurocognitive benefits of flash radiotherapy driven by reduced reactive oxygen species. *Proc. Natl. Acad. Sci.* **116**, 10943–10951, DOI: 10.1073/pnas.1901777116 (2019). https://www.pnas.org/content/116/22/10943.full.pdf.
11. Town, C. D. Radiobiology. effect of high dose rates on survival of mammalian cells. *Nature* **215**, 847–848, DOI: https://doi.org/10.1038/215847a0 (1967).

12. Berry, R. J., Hall, E. J., Forster, D. W., Storr, T. H. & Goodman, M. J. Survival of mammalian cells exposed to x rays at ultra-high dose-rates. *Br. J. Radiol.* **42**, 102–107, DOI: https://doi.org/10.1259/0007-1285-42-494-102 (1969).

13. Favaudon, V. *et al.* Ultrahigh dose-rate FLASH irradiation increases the differential response between normal and tumor tissue in mice. *ence Transl. Medicine* **6**, 245ra93, DOI: https://doi.org/10.1126/scitranslmed.3008973 (2014).

14. Montay-Gruel, P. *et al.* Hypo-fractionated flash-rt as an effective treatment against glioblastoma that reduces neurocognitive side effects in mice. *Clin. Cancer Res.* DOI: https://doi.org/10.1158/1078-0432.CCR-20-0894 (2020). https://clincancerres.aacrjournals.org/content/early/2020/10/15/1078-0432.CCR-20-0894.full.pdf.

15. Venkatesulu, B. P., Sharma, A., Pollard-Larkin, J. M., Sadagopan, R. & Krishnan, S. Ultra high dose rate (35 Gy/sec) radiation does not spare the normal tissue in cardiac and splenic models of lymphopenia and gastrointestinal syndrome. *Sci. Reports* **9**, DOI: https://doi.org/10.1038/s41598-019-53562-y (2019).

16. Chabi, S. *et al.* Ultra-high dose rate FLASH and conventional dose rate irradiation differentially affect human acute lymphoblastic leukemia and normal hematopoiesis. *Int. J. Radiat. Oncol.* DOI: https://doi.org/10.1016/j.ijrobp.2020.10.012 (2020).

17. Soto, L. A., Casey, K. M., Wang, J., Blaney, A. & Loo, B. W. Flash irradiation results in reduced severe skin toxicity compared to conventional-dose-rate irradiation. *Radiat. Res.* DOI: https://doi.org/10.1667/RADE-20-00090 (2020).

18. Pierre, M. G. *et al.* X-rays can trigger the flash effect: Ultra-high dose-rate synchrotron light source prevents normal brain injury after whole brain irradiation in mice. *Radiother. Oncol.* **129**, 582–588, DOI: https://doi.org/10.1016/j.radonc.2018.08.016 (2018).

19. Loo, B. W. *et al.* (p003) delivery of ultra-rapid flash radiation therapy and demonstration of normal tissue sparing after abdominal irradiation of mice. *Int. J. Radiat. Oncol.* **98**, DOI: https://doi.org/10.1016/j.ijrobp.2017.02.101 (2017).

20. Montay-Gruel *et al.* Irradiation in a flash: Unique sparing of memory in mice after whole brain irradiation with dose rates above 100 Gy/s. *Radiother. Oncol.* DOI: https://doi.org/10.1016/j.radonc.2017.05.003 (2017).

21. Marie-Catherine, V. *et al.* The advantage of FLASH radiotherapy confirmed in mini-pig and cat-cancer patients. *Clin. Cancer Res. An Off. J. Am. Assoc. for Cancer Res.* clincanres.3375.2017, DOI: https://doi.org/10.1158/1078-0432.CCR-17-3375 (2018).

22. Levy, K., Rafat, M., Casey, K. & Rankin, E. Total abdominal ultra-rapid flash irradiation decreases gastrointestinal toxicity compared to conventional radiation. *Gynecol. Oncol.* **154**, 75, DOI: https://doi.org/10.1016/j.ygyno.2019.04.177 (2019).

23. Bourhis, J., Sozzi, W. J., Jorge, P. G., Gaide, O. & Vozenin, M. C. Treatment of a first patient with FLASH-radiotherapy. *Radiother. Oncol.* **139**, DOI: https://doi.org/10.1016/j.radonc.2019.06.019 (2019).

24. Medical, V. Feasibility study of FLASH radiotherapy for the treatment of symptomatic bone metastases (fast-01). [EB/OL]. https://clinicaltrials.gov/ct2/show/study/NCT04592887, October 19, 2020.

25. Vozenin, M.-C., Hendry, J. & Limoli, C. Biological benefits of ultra-high dose rate flash radiotherapy: Sleeping beauty awoken. *Clin. Oncol.* **31**, 407 – 415, DOI: https://doi.org/10.1016/j.clon.2019.04.001 (2019).

26. Fouillade, C. *et al.* Flash irradiation spares lung progenitor cells and limits the incidence of radio-induced senescence. *Clin. Cancer Res.* **26**, 1497–1506, DOI: 10.1158/1078-0432.CCR-19-1440 (2020). https://clincancerres.aacrjournals.org/content/26/6/1497.full.pdf.

27. Simmons, D. A., Lartey, F. M., Schüler, E., Rafat, M. & Loo, B. W. Reduced cognitive deficits after flash irradiation of whole mouse brain are associated with less hippocampal dendritic spine loss and neuroinflammation. *Radiother. Oncol.* **139**, 4–10, DOI: https://doi.org/10.1016/j.radonc.2019.06.006 (2019).

28. B, J. B. A. *et al.* Clinical translation of flash radiotherapy: Why and how? *Radiother. Oncol.* **139**, 11–17, DOI: https://doi.org/10.1016/j.radonc.2019.04.008 (2019).

29. Smyth, L. M. *et al.* Comparative toxicity of synchrotron and conventional radiation therapy based on total and partial body irradiation in a murine model. *Sci. reports* **8**, DOI: https://doi.org/10.1038/s41598-018-30543-1 (2018).

30. Zlobinskaya *et al.* The effects of ultra-high dose rate proton irradiation on growth delay in the treatment of human tumor xenografts in nude mice. *Radiat. research* **181**, 177–183, DOI: https://doi.org/10.1667/RR13464.1 (2014).

31. Beyreuther, E. *et al.* Feasibility of proton flash effect tested by zebrafish embryo irradiation. *Radiother. Oncol.* **139**, 46 – 50, DOI: https://doi.org/10.1016/j.radonc.2019.06.024 (2019). FLASH radiotherapy International Workshop.

32. Rama, N. *et al.* Improved tumor control through t-cell infiltration modulated by ultra-high dose rate proton flash using a clinical pencil beam scanning proton system. *Int. J. Radiat. Oncol.* **105**, S164–S165, DOI: https://doi.org/10.1016/j.ijrobp.2019.06.187 (2019).

33. Feng, G. *et al.* Design and calculation of Flash-RT based on PARTER. *Chin. J. Med. Phys.* **37**, 1081–1087, DOI: https://doi.org/10.3969/j.issn.1005-202X.2020.09.001 (2020).

34. Hirayama, R., Furusawa, Y., Fukawa, T. & Ando, K. Repair kinetics of dna-dsb induced by x-rays or carbon ions under oxic and hypoxic conditions. *J. radiation research* **46**, 325–332, DOI: https://doi.org/10.1269/jrr.46.325 (2005).

35. Gerweck, L. E., Richards, B. & Jennings, M. The influence of variable oxygen concentration on the response of cells to heat or x irradiation. *Radiat. research* **85**, 314–320, DOI: https://doi.org/10.2307/3575564 (1981).

36. Ling, C. C., Michaels, H. B., Gerweck, L. E., Epp, E. R. & Peterson, E. C. Oxygen sensitization of mammalian cells under different irradiation conditions. *Radiat. research* **86**, 325–340, DOI: https://doi.org/10.2307/3575509 (1981).

37. Spiro, I. J., Ling, C. C., Stickler, R. & Gaskill, J. Oxygen radiosensitisation at low dose rate. *The Br. J. Radiol.* **58**, 357–363, DOI: https://doi/abs/10.1259/0007-1285-58-688-357 (1985).

38. Ling, C. C., Spiro, I. J., Mitchell, J. & Stickler, R. The variation of oer with dose rate. *Int. J. Radiat. Oncol. Biol. Phys.* **11**, 1367–1373, DOI: https://doi.org/10.1016/0360-3016(85)90253-6 (1985).

39. Booth, C., Tudor, G., Tudor, J., Katz, B. & MacVittie, T. Acute gastrointestinal syndrome in high-dose irradiated mice. *Heal. Phys.* **103**, 383–399, DOI: 10.1097/HP.0b013e318266ee13 (2012).

40. Hanson, W. R. *et al.* Comparison of intestine and bone marrow radiosensitivity of the balb/c and the c57bl/6 mouse strains and their b6cf1 offspring. *Radiat. Res.; (United States)* DOI: 10.2307/3577002.

41. Mukherjee, S., Sainis, K. & Deobagkar, D. D. F 1 hybrids of balb/c and c57bl/6 mouse strains respond differently to low-dose ionizing radiation exposure. *J. genetics* **93**, 667–682 (2014).

42. Zhang, Q. *et al.* Flash investigations using protons: Design of delivery system, preclinical setup and confirmation of flash effect with protons in animal systems. *Radiat. Res.* DOI: https://doi.org/10.1667/RADE-20-00068.1 (2020).

43. Agostinelli, S. *et al.* Geant4—a simulation toolkit. *Nucl. Instruments Methods Phys. Res. Sect. A: Accel. Spectrometers, Detect. Assoc. Equip.* **506**, 250 – 303, DOI: https://doi.org/10.1016/S0168-9002(03)01368-8 (2003).

44. Spitz, D. R. *et al.* An integrated physico-chemical approach for explaining the differential impact of flash versus conventional dose rate irradiation on cancer and normal tissue responses. *Radiother. Oncol.* **139**, 23–27, DOI: https://doi.org/10.1016/j.radonc.2019.03.028 (2019).

45. Pratx, G. & Kapp, D. S. A computational model of radiolytic oxygen depletion during FLASH irradiation and its effect on the oxygen enhancement ratio. *Phys. Medicine & Biol.* **64**, 185005, DOI: 10.1088/1361-6560/ab3769 (2019).

46. Pratx, G. & Kapp, D. S. Ultra-high-dose-rate flash irradiation may spare hypoxic stem cell niches in normal tissues. *Int. J. Radiat. Oncol.* **105**, 190–192, DOI: https://doi.org/10.1016/j.ijrobp.2019.05.030 (2019).

47. Xie, W. *et al.* Comparison of direct DNA strand break simulated with different DNA models. *Radiat. Prot. Dosim.* **156**, 283–288, DOI: https://doi.org/10.1093/rpd/nct074 (2013). https://academic.oup.com/rpd/article-pdf/156/3/283/4526990/nct074.pdf.

48. Junli *et al.* Dna strand breaks induced by electrons simulated with nanodosimetry monte carlo simulation code: Nasic. *Radiat. Prot. Dosim.* DOI: https://doi.org/10.1093/rpd/ncv171 (2015).

49. Chen, Y., Li, C. & Li, J. Radiosensitization effect of the gold nanoparticle in the cell simulated with nasic code (2017).

50. Li, W. *et al.* Intercomparison of dose enhancement ratio and secondary electron spectra for gold nanoparticles irradiated by x-rays calculated using multiple monte carlo simulation codes. *Phys. Medica* **69**, 147 – 163, DOI: https://doi.org/10.1016/j.ejmp.2019.12.011 (2020).

51. Zhu, H. *et al.* Modeling of cellular response after flash irradiation: a quantitative analysis based on the radiolytic oxygen depletion hypothesis. *under review* (2020).

52. Zhu, H. *et al.* Modeling the oxygen effect on cellular responses following exposure to ionizing radiation. *under review* (2020).

Acknowledgements

This work was supported by National Natural Science Foundation of China with grant (11975218, 11905210, 11805192, 12005211 and 11605190), Innovation Foundation of CAEP with grant (CX2019036, CX2019037).

Author contributions statement

Y.Y., X.D., F.G., and D.W. conceived the investigation; X.D., F.G., Y.Y., D.W. and H.Z. designed the study; J.W., D.X., Z.Z. T.D.,Y.Z.,G.F.,J.L.,B.L., K.Z., P.L., X.S., H.W., L.Y., C.L., M.L., Y.L., M.C. and J.Z. conducted the experiments; F.G., Y.Y. performed data analysis and H.Z. carried out simulations; F.G., Y.Y., H.Z., D.W. and X.D. interpreted the results; G.X. and Q.K. observed the morphological changes of mice's tissue under the microscope;Y.Y., F.G., H.Z., D.W., Z.Z., and X.D. contributed to writing the manuscript; X.D. and D.W. provided overall supervision. All authors reviewed the manuscript.

Competing interests

The authors declare no competing interests.

Additional information

To include, in this order: **Accession codes** (where applicable); **Competing interests** (mandatory statement).

The corresponding author is responsible for submitting a competing interests statement on behalf of all authors of the paper. This statement must be included in the submitted article file.

Supplementary

Theoretic analysis of the FLASH effect of different pulse fractionations

Three pulse fractionation regimens, i.e., a total dose of 20 Gy delivered to the target tissue in 1, 2, or 4 fractions, were considered for analysis. Fig. S1a shows the rapid oxygen depletion due to FLASH irradiation and the recovery of pO_2 due to oxygen diffusion from blood vessels after each fraction. Fig. S1b shows that the pO_2 values drop to the lowest level within the time scale of 40 μs, the low pO_2 level can hold for approximately 10 ms, and the oxygen tension in tissues is generally fully recovered within 1 second.

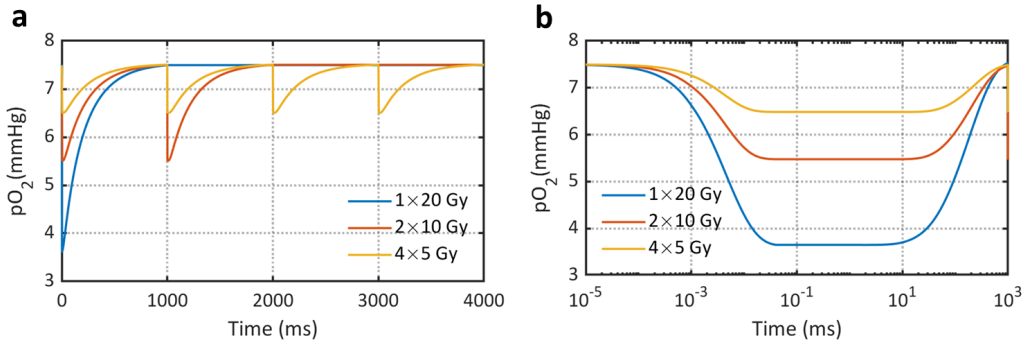

Figure S1. Dynamic change of pO_2 in cells that were exposed to HEX FLASH radiation with a total dose of 20 Gy delivered in 1, 2, and 4 fractions. **a** Dynamic change of pO_2 in cells after each fraction; **b** Semi-log plot of dynamic change of pO_2 in cells after the first fraction.

Different fractionations of FLASH irradiation resulted in differences of pO_2 evolution after each pulse, the pO_2 value after each pulse dominates the indirect DNA damage yield as well as cell SFs. Table S1 shows the cellular responses of CHO cells toward different FLASH irradiation schedules. The pO_2 value after the irradiation of 20 Gy in 1 fraction of was 45.1% lower than that after the irradiation of 20 Gy delivered in 4 fractions, and this further led to 13.5% less indirect DNA damages and 75.6% higher cell SF.

Table S1. The pO_2 value after each pulse, indirect DNA damage yield, and cell SFs of CHO cells (pO_2 =7.5 mmHg) were exposed to CTFEL X-ray FLASH radiation with a total dose of 20 Gy delivered in 1, 2, and 4 fractions.

Fractionation	The pO_2 value after each pulse (mmHg)	Indirect DNA damage yield ($Gbp^{-1}Gyp^{-1}$)	Cell SFs
1×20 Gy	3.58	4.82	0.47%
2×10 Gy	5.54	5.37	0.16%
4×5 Gy	6.52	5.57	0.10%
Max. rel. diff.*	45.1%	13.5%	75.6%

* Max. rel. diff: maximum relative difference was calculated with (1-min./max.)$\times$100%

Second experiment

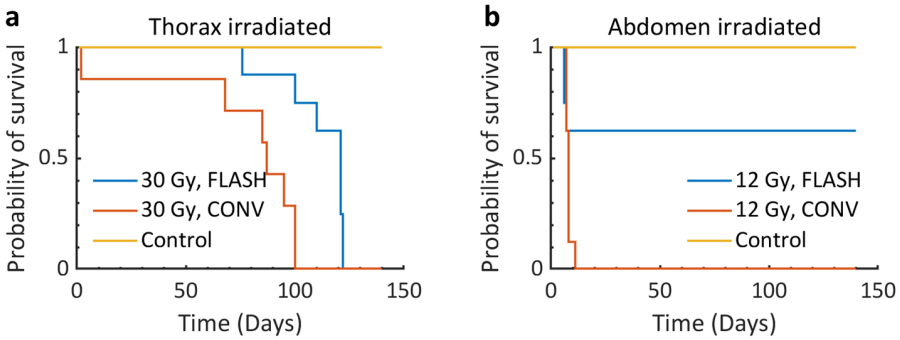

Figure S2. **a** Survival curves of healthy BAL b/c mice of the control group, after 30 Gy FLASH, and 30 Gy CONV irradiation at thorax. **b** Survival curves of healthy BAL b/c mice of the control group, after 12 Gy FLASH, and 12 Gy CONV irradiation at abdomen. P values were derived from one-way repeated ANOVA: ****$P < 0.0001$.